End-point trajectory shaping based on an arbitrary vector for feedforward control of muscular internal forces

Matsutani, Yuki
Department of Intelligent Mechanical Engineering, Fukuoka Institute of Technology

Tahara, Kenji
Department of Mechanical Engineering, Faculty of Engineering, Kyushu University

Kino, Hitoshi
Department of Mechanical and System Engineering, Chukyo University

出版情報：ROBOMECH Journal. 13 (1), pp.8-, 2026-04-10. Springer
バージョン：

Matsutani *et al. ROBOMECH Journal* (2026) 13:8
https://doi.org/10.1186/s40648-026-00334-9

ROBOMECH Journal

RESEARCH Open Access

End-point trajectory shaping based on an arbitrary vector for feedforward control of muscular internal forces

Yuki Matsutani[1*], Kenji Tahara[2†] and Hitoshi Kino[3†]

Abstract

Current research has focused on developing robots that can imitate the musculoskeletal structure of human body to achieve skillful movements similar to those of a human. Several studies have investigated the end-point trajectory of musculoskeletal systems, but a sensor is essential for trajectory tracking. The previously proposed muscular internal force feedforward control method achieves point-to-point convergence to a desired position without any sensor; however, it lacks explicit control over the specific end-point trajectory from the initial to the desired position. Given that the end-point trajectory depends on the shape of the potential field generated by the control input, the trajectory sometimes takes a detour depending on how the desired position is set. To resolve this limitation, in this study, a novel shaping method is proposed for the end-point trajectory of musculoskeletal systems using the muscle redundancy. The end-point trajectory is shaped by optimizing a control input that cannot be uniquely determined due to the muscle redundancy based on the objective function of joint torques. As an advantage in the proposed method, the end-point trajectory can be shaped without sensors. Furthermore, the control input can be prevented from saturating the output limit by formulating the problem as a constrained minimization problem. The effectiveness of the proposed method is presented using simulation results. The proposed method definitely converges at the desired position without depending on the shaping result of the end-point trajectory because the target is a musculoskeletal system with muscular arrangements that converge to the desired position.

Keywords Musculoskeletal system, Feedforward control method, End-point trajectory, Optimization problem

Introduction

The musculoskeletal structure of the human body comprises muscles, bones, and joints. Further, joint angles can be modified through muscle contractions, while joint stiffness can be varied by adjusting the internal forces of the muscles. These characteristics enable skillful movements, e.g., precise object handling and heavy lifting.

In robotics, current research has focused on developing robots that can imitate the musculoskeletal structure to achieve skillful movements similar to those of a human. For example, Wittmeier et al. [1] developed anthropomimetic robots with more than forty muscles that imitate

†Kenji Tahara and Hitoshi Kino have contributed equally to this work.

*Correspondence:
Yuki Matsutani
matsutani@fit.ac.jp
[1]Department of Intelligent Mechanical Engineering, Fukuoka Institute of Technology, 3-30-1 Wajiro-higashi, Higashi-ku, Fukuoka, Fukuoka 8110295, Japan
[2]Department of Mechanical Engineering, Faculty of Engineering, Kyushu University, 744 Moto'oka, Nishi-ku, Fukuoka, Fukuoka 8190395, Japan
[3]Department of Mechanical and System Engineering, Chukyo University, 101-2 Yagoto Honmachi, Showa-ku, Nagoya, Aichi 4668666, Japan

the structure of the human torso. Further, Wittmeier et al. developed a computed force control method for those robots and demonstrated the accurate tracking of a desired trajectory in a joint space Jantsch et al. [2]. Inaba et al. developed whole-body musculoskeletal humanoids (Kotaro [3], Kojiro [4], Kenshiro [5], and Kengoro [6]) and realized flexible movements. Morizono et al. [7] proposed a new musculoskeletal robot that eliminates the need for motors on the moving parts of a serial-link mechanism, demonstrating its potential for high-speed movement. These studies indicated that robots designed based on the principles of the human body structure can achieve movements that are difficult to perform for conventional robots.

Previously, the authors proposed a muscular internal force feedforward control method for a musculoskeletal system to reproduce dexterous, human-like movements [8, 9]. In this method, the internal force balancing at the desired position is the control input. A unique potential field is generated when an internal force is applied. If the stable equilibrium point of this potential field agrees with the desired position, the movement of the musculoskeletal system converges at the desired position, and the proposed method realizes senseless positioning. However, this method adopts a point-to-point (PTP) approach that ensures convergence to the desired position but does not control the end-point trajectory from the initial position.

Tahara et al. [10] proposed an iterative learning control method that uses multiple space variables. Their method enables tracking a desired trajectory even if the sensor information includes errors because the feedback and feedforward inputs construct the task-space and muscle-space information, respectively. Blana et al. [11] proposed a control method based on an inverse dynamics model and achieved high-accuracy trajectory. Liu et al. [12] proposed an intelligent controller, based on an evolutionary diagonal recurrent neural network, for the musculoskeletal system to achieve accurate tracking. Katayama et al. [13] proposed a parallel-hierarchical neural network model as an extension of a feedback-error-learning scheme and achieved high tracking controllability. Kawato et al. proposed the feedback-error-learning scheme [14] as a trajectory control method for a serial link robot. Thus, the trajectory control method for a serial link robot can be extended to the musculoskeletal system by converting the control input to each muscular tension. For example, serial link robots leveraging the iterative learning control scheme proposed by Arimoto [15] can follow a desired trajectory. Wang et al. [16] proposed a trajectory control method based on the joint viscoelasticity and achieved high-accuracy control. Therefore, two control methods can be used for the musculoskeletal system. However, to implement these methods, a sensor is required to include the feedback control. Kinjo et al. [17] proposed a continuous path control method that amplified muscular internal force feedforward control. Their method controls end-point trajectory by optimizing the muscular internal force for generating the potential field that can achieve the desired trajectory; however, this method cannot accurately follow all trajectories within the movable range because the muscular internal force cannot always generate the required potential field. Senda et al. [18] addressed this limitation using a control method that combined the approach reported by Kinjo et al. [17] with an iterative learning method. The method devised by Senda et al. improves trajectory trackability by iteratively learning an initial joint angular velocity and joint viscosity. However, this method requires joint angle sensors, and during experiments, the joint viscosity must change in response to the end-point trajectory.

The muscular internal force feedforward positioning method proposed in previous research [8, 9] is a PTP control approach. Further, this method cannot control the end-point trajectory from the initial point to the desired point, and therefore, the path taken by the end-point remains unclear. The end-point trajectory is affected by the shape of the potential field generated by the muscular internal force, which depends on muscular arrangements and an arbitrary vector. Therefore, this paper introduces a shaping method for the end-point trajectory; this proposed method uses the arbitrary vector for the musculoskeletal system with muscular arrangements that converge to the desired position. Ideally, the end-point trajectory should accurately follow a desired trajectory. However, continuous path (CP) control based on the muscular internal force feedforward positioning cannot accurately realize the desired trajectory for the following reasons.

- Muscles within the musculoskeletal system can generate only tensile force.
- End-point trajectory depends on the arbitrary vector and muscular arrangements.
- In this study, the arbitrary vector is modified while the convergence of the desired position is ensured as muscular arrangements affect the convergence.
- There is an output limit for muscular tension that corresponds to the maximum value of a motor output when executing an experiment.

The proposed method shapes the end-point trajectory by optimizing an arbitrary vector based on an objective function that comprises joint torques at any end-point position. There are several calculation methods of the joint torque at any end-point position. In the proposed method, the torque is computed by using the computed torque method [19] to consider the effect of the inertia

of the musculoskeletal system and set the valid desired joint torque. Then, the computed torque method can be utilized without modification for the CP control of the musculoskeletal system. However, in practical applications, it is challenging for the computed torque method to accurately converge to the desired position due to physical modeling errors and disturbances. It is possible to decrease those influences by adding a servo compensator, provided that this method requires a sensor. When converting the control input of the computed torque method into individual muscle inputs, the method cannot be directly applied, as the resulting inputs may exceed the allowable range, leading to possible instability. By contrast, the proposed method does not affect the convergence of the desired position because the convergence is secured by the muscular arrangements. The proposed method is affected by modeling errors in the muscular arrangement; however, this effect is expected to be less significant because the muscular arrangement can be measured with relative ease. Another advantage of the proposed method is that the control input is computed within the allowable motor input range. In the proposed method, the system does not become unstable even under disturbances during motion because the control input is a step input. Therefore, the proposed method can shape the end-point trajectory without requiring a sensor and outperforms the computed torque method in terms of convergence.

The remainder of this paper is organized as follows: Section 2 explains the musculoskeletal system, which is a controlled object; Section 3 presents the muscular internal force feedforward positioning; Section 4 proposes the novel shaping method of the end-point trajectory using the arbitrary vector; Section 5 presents the effectiveness of the proposed method using simulation results; Section 6 evaluates the isotropism of the proposed method; and Section 7 concludes the paper.

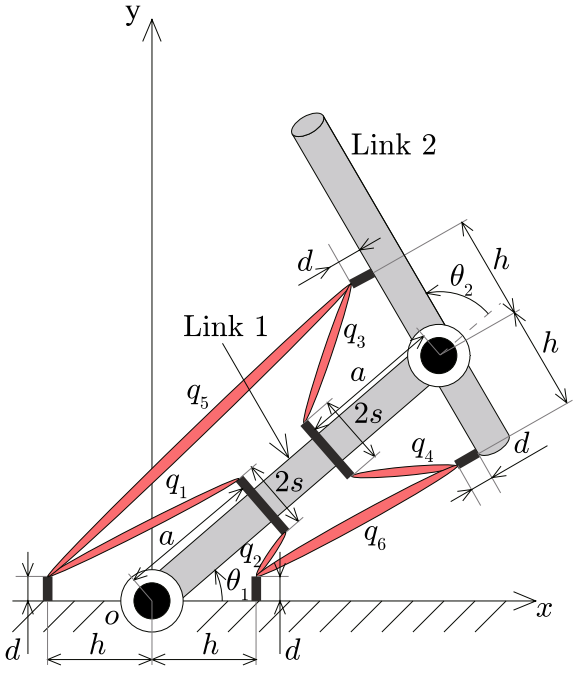

Fig. 1 Musculoskeletal system composed of two links and six muscles

Musculoskeletal system

The musculoskeletal system shown in Fig. 1 is a controlled object designed to imitate the upper arm of a human. This system has a planar two-link manipulator and possesses six muscles. Each link is driven solely by muscles because the two joints do not have any motor. Further, in this system, muscles can generate only a tensile force, and therefore, a movement of the joint with one degree of freedom requires at least two muscles. This system possesses two biarticular muscles ($\boldsymbol{q}_5$, $\boldsymbol{q}_6$) characteristic of the musculoskeletal structure. It is characterized by drive redundancy because the planar two-link manipulator possesses six muscles as the driving source. In the experimental device [20], the muscles consist of a combination of wires and motors instead of muscle actuators. For simplicity, we assume that the movement of the muscle mass is negligible and that the muscles contract linearly. Moreover, we assume that the movement is not affected by gravity because it is set within a horizontal plane.

Relationship between muscle and joint spaces

The relationship between the muscle length vector $\boldsymbol{q}(t) \in \mathbb{R}^6$ and joint angle vector $\boldsymbol{\theta}(t) \in \mathbb{R}^2$ of the musculoskeletal system shown in Fig. 1 is represented by

$$\boldsymbol{q}(t) = \boldsymbol{g}(\boldsymbol{\theta}(t)), \tag{1}$$

where $\boldsymbol{g}(\boldsymbol{\theta}(t))$ represents a nonlinear function. Differentiating this with respect to time yields

$$\dot{\boldsymbol{q}}(t) = -\boldsymbol{W}(\boldsymbol{\theta}(t))^{\mathrm{T}}\dot{\boldsymbol{\theta}}(t), \tag{2}$$

where $\dot{\boldsymbol{q}}(t) \in \mathbb{R}^6$, $\dot{\boldsymbol{\theta}}(t) \in \mathbb{R}^2$, and $-\boldsymbol{W}(\boldsymbol{\theta}(t))^{\mathrm{T}} \in \mathbb{R}^{6\times 2}$ represent a muscular contraction speed vector, joint angular velocity vector, and Jacobian matrix that expresses a relationship between $\dot{\boldsymbol{q}}(t)$ and $\dot{\boldsymbol{\theta}}(t)$, respectively.

According to the principle of virtual work, the relationship between a joint torque vector $\boldsymbol{\tau}(t) \in \mathbb{R}^2$ and muscular tension vector $\boldsymbol{\alpha}(t) \in \mathbb{R}^6$ is represented by

$$\boldsymbol{\tau}(t) = \boldsymbol{W}(\boldsymbol{\theta}(t))\boldsymbol{\alpha}(t). \tag{3}$$

Using a pseudo inverse matrix $\boldsymbol{W}(\boldsymbol{\theta}(t))^{+} \in \mathbb{R}^{6\times 2}$, a general solution of this equation can be represented as

$$\boldsymbol{\alpha}(t) = \boldsymbol{W}(\boldsymbol{\theta}(t))^{+}\boldsymbol{\tau}(t) + \left(\boldsymbol{I}_6 - \boldsymbol{W}(\boldsymbol{\theta}(t))^{+}\boldsymbol{W}(\boldsymbol{\theta}(t))\right)\boldsymbol{k_e}, \quad (4)$$

where $\boldsymbol{I}_6 \in \mathbb{R}^{6\times 6}$ and $\boldsymbol{k_e} \in \mathbb{R}^6$ represent a unit matrix and an arbitrary vector, respectively. This equation indicates the tensile force $\boldsymbol{\alpha}(t)$ necessary for generating the joint torque $\boldsymbol{\tau}(t)$. The second term in Eq. (4) represents the internal force composition that does not generate the joint torque. The muscular internal force vector $\boldsymbol{v}(\boldsymbol{\theta}(t)) \in \mathbb{R}^6$ is defined as

$$\boldsymbol{v}(\boldsymbol{\theta}(t)) = \left(\boldsymbol{I}_6 - \boldsymbol{W}(\boldsymbol{\theta}(t))^{+}\boldsymbol{W}(\boldsymbol{\theta}(t))\right)\boldsymbol{k_e}. \quad (5)$$

Relationship between task and joint spaces

The relationship between an end-point position vector $\boldsymbol{x}(t) = [x(t),\ y(t)]^{\mathrm{T}}$ and joint angle vector $\boldsymbol{\theta}(t) = [\theta_1(t),\ \theta_2(t)]^{\mathrm{T}}$ of the musculoskeletal system as shown in Fig. 1 is represented by

$$\begin{bmatrix} x(t) \\ y(t) \end{bmatrix} = \begin{bmatrix} l_1 \cos\theta_1(t) + l_2 \cos\left(\theta_1(t) + \theta_2(t)\right) \\ l_1 \sin\theta_1(t) + l_2 \sin\left(\theta_1(t) + \theta_2(t)\right) \end{bmatrix}, \quad (6)$$

where l_1 and l_2 represent a link length. Differentiating this equation with time yields

$$\dot{\boldsymbol{x}}(t) = \boldsymbol{J}(t)\dot{\boldsymbol{\theta}}(t), \quad (7)$$

where $\dot{\boldsymbol{x}}(t) \in \mathbb{R}^2$ and $\boldsymbol{J}(t) \in \mathbb{R}^{2\times 2}$ represent an end-point velocity vector and a Jacobian matrix, respectively. Further, by differentiating Eq. (7) with respect to time, the relationship between an end-point acceleration vector $\ddot{\boldsymbol{x}}(t) \in \mathbb{R}^2$ and joint angular acceleration vector $\ddot{\boldsymbol{\theta}}(t) \in \mathbb{R}^2$ can be expressed as

$$\ddot{\boldsymbol{x}}(t) = \dot{\boldsymbol{J}}(t)\dot{\boldsymbol{\theta}}(t) + \boldsymbol{J}(t)\ddot{\boldsymbol{\theta}}(t). \quad (8)$$

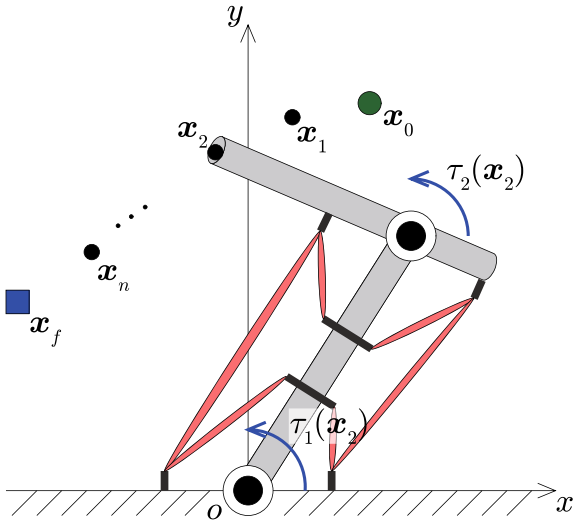

Fig. 2 Desired joint torque at any end-point position

Equation of motion

An equation of motion of the musculoskeletal system based on the planar two-link manipulator shown in Fig. 1 is given by

$$\boldsymbol{\tau}(t) = \boldsymbol{M}(\boldsymbol{\theta}(t))\ddot{\boldsymbol{\theta}}(t) + \boldsymbol{h}(\boldsymbol{\theta}(t), \dot{\boldsymbol{\theta}}(t)) + \boldsymbol{D}\dot{\boldsymbol{\theta}}(t), \quad (9)$$

where $\boldsymbol{M}(\boldsymbol{\theta}(t)) \in \mathbb{R}^{2\times 2}$, $\boldsymbol{h}(\boldsymbol{\theta}(t), \dot{\boldsymbol{\theta}}(t)) \in \mathbb{R}^2$, and $\boldsymbol{D} \in \mathbb{R}^{2\times 2}$ represent an inertia matrix, non-linear term, and joint viscosity matrix, respectively.

Muscular internal force feedforward positioning

The control method for the musculoskeletal system uses the muscular internal force feedforward positioning proposed by Kino et al. [8, 9]. In this method, the internal force $\boldsymbol{v}(\boldsymbol{\theta}_d) \in \mathbb{R}^6$ balancing the desired position $\boldsymbol{\theta}_d \in \mathbb{R}^2$ is input into muscular tension $\boldsymbol{\alpha}(t)$.

$$\boldsymbol{\alpha}(t) = \boldsymbol{v}(\boldsymbol{\theta}_d) \quad (10)$$

$$= \left(\boldsymbol{I}_6 - \boldsymbol{W}(\boldsymbol{\theta}_d)^{+}\boldsymbol{W}(\boldsymbol{\theta}_d)\right)\boldsymbol{k_e}. \quad (11)$$

The Jacobian matrix, calculated using the desired position, is a constant as it does not vary with the joint angle. In this study, the elements of the arbitrary vector are set as constants. Therefore, the desired internal force has a constant value, serving as the step input. The desired muscular internal force $\boldsymbol{v}(\boldsymbol{\theta}_d)$ does not generate the joint torque $\boldsymbol{\tau}(t)$ when $\boldsymbol{\theta}(t) = \boldsymbol{\theta}_d$ because the muscular internal force $\boldsymbol{v}(\boldsymbol{\theta}(t))$ has an internal force composition that does not generate the joint torque $\boldsymbol{\tau}(t)$.

$$\boldsymbol{\tau}(t) = \boldsymbol{W}(\boldsymbol{\theta}_d)\boldsymbol{v}(\boldsymbol{\theta}_d) = 0. \quad (12)$$

However, the desired muscular internal force $\boldsymbol{v}(\boldsymbol{\theta}_d)$ may generate the joint torque when $\boldsymbol{\theta}(t) = \boldsymbol{\phi}\ (\neq \boldsymbol{\theta}_d)$ because the desired muscular internal force $\boldsymbol{v}(\boldsymbol{\theta}_d)$ may not agree with the internal force composition $\boldsymbol{v}(\boldsymbol{\phi})$.

$$\boldsymbol{\tau}(t) = \boldsymbol{W}(\boldsymbol{\phi})\boldsymbol{v}(\boldsymbol{\theta}_d) \neq 0. \quad (13)$$

Muscular internal force positioning is controlled using this characteristic.

An original potential field is generated by inputting the desired muscular internal force $\boldsymbol{v}(\boldsymbol{\theta}_d)$. If this potential field is shaped as a stable equilibrium point at the desired position, the movement of the musculoskeletal system converges on the desired position. Given that the desired internal force is the step input, the potential P in a joint angle coordinate can be calculated by multiplying the muscle length vector by the desired internal force vector.

$$P(\boldsymbol{\theta}(t)) = \left(\boldsymbol{q}(\boldsymbol{\theta}(t)) - \boldsymbol{q}(\boldsymbol{\theta}_d)\right)^{\mathrm{T}}\boldsymbol{v}(\boldsymbol{\theta}_d), \quad (14)$$

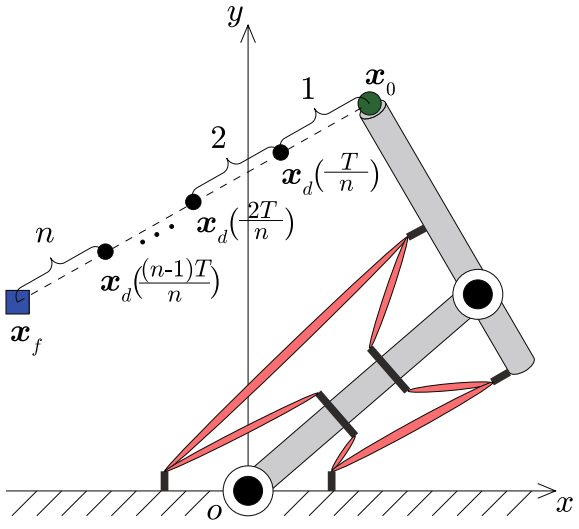

Fig. 3 Method for setting the desired joint torque and the end-point positions

where $\boldsymbol{q}(\boldsymbol{\theta}_d)$ represents a muscle length vector at the desired position. The muscle length is determined by the joint angle and muscular arrangements, and the desired muscular internal force is determined using these factors and the arbitrary vector. The end-point trajectory and convergence of muscular internal force feedforward positioning depends on these factors because the shape of the potential field depends on the muscular arrangements and arbitrary vector. The relationship between the convergence and muscular arrangement have been analyzed in previous research [9, 20].

Shaping method of end-point trajectory using arbitrary vector

Muscular internal force feedforward positioning [8, 9] is a PTP control method that focuses on convergence at the desired position. The trajectory from the initial position to the desired position is not controlled, and therefore, the end-point trajectory depends on the shape of the potential field. This study proposes a novel shaping method of the end-point trajectory without using sensors and by employing muscular internal force feedforward positioning.

The proposed method shapes the end-point trajectory using the arbitrary vector $\boldsymbol{k_e}$ that affects the shape of the potential field. Meanwhile, the following characteristics need to be considered in muscular internal force feedforward positioning.

- The musculoskeletal muscles generate only tensile force.
- The shape of the potential field depends on not only the arbitrary vector $\boldsymbol{k_e}$ but also muscular arrangements. The end-point trajectory is affected by muscular arrangements, which are fixed parameters that confirmed the convergence of the desired position in previous research.
- There is an output limit of muscular tension because there is a maximum value of the motor output in the experiment device.

Table 1 Physical parameters of the musculoskeletal system used for the simulations

	Link 1	Link 2
Mass [kg]	1.678	0.95
Length [m]	0.315	0.234
Center of gravity [m]	0.1575	0.117
Moment of inertia [kgm^2]	0.011	0.004
Joint viscosity [Ns/rad]	1.0	1.0

Table 2 Muscular arrangement of the musculoskeletal system used for the simulations

	a	*d*	*h*	*s*
value [mm]	120	20	50	10

Consequently, ensuring that the end-point trajectories precisely follow the desired trajectory solely by employing the arbitrary vector $\boldsymbol{k_e}$ is challenging. Therefore, this paper proposes a novel shaping method for end-point trajectory that optimizes the arbitrary vector $\boldsymbol{k_e}$.

The proposed method sets the desired joint torque $\boldsymbol{\tau}_d(\boldsymbol{x}_i) \in \mathbb{R}^2$ generated at any end-point position $\boldsymbol{x}_i$ $(i = 1, 2, \ldots, n)$ on the desired trajectory (Fig. 2). Further, the end-point trajectory shapes the desired trajectory by optimizing the arbitrary vector $\boldsymbol{k_e}$ to realize the desired joint torque $\boldsymbol{\tau}_d(\boldsymbol{x}_i)$. The optimization method of the arbitrary vector involves finding a minimum solution of an object function using the Nelder–Mead method [21] that includes an augmented Lagrangian function for constrained minimization problems and converts it to an unconstrained optimization problem.

Object function

Equation (11) is substituted into Eq. (3) to set the object function as

$$\boldsymbol{\tau}(\boldsymbol{x}(t)) = \boldsymbol{W}(\boldsymbol{x}(t)) \left(\boldsymbol{I}_6 - \boldsymbol{W}(\boldsymbol{x}_d(t))^{+}\boldsymbol{W}(\boldsymbol{x}_d(t))\right) \boldsymbol{k_e}, \quad (15)$$

$$= \boldsymbol{Q}(\boldsymbol{x}(t))\boldsymbol{k_e}, \quad (16)$$

where the variables represent the task space because the end-point trajectory is presented in the task space. The necessary joint angle vector is calculated by an inverse relationship of Eq. (6) using the end-point position vector. Then, using the desired joint torque $\boldsymbol{\tau}_d(\boldsymbol{x}_i)$ to realize the desired trajectory, the object function $f(\boldsymbol{k_e})$ is defined as

$$f(\boldsymbol{k_e}) = \sum_{i=1}^{n} \|\boldsymbol{\tau}_d(\boldsymbol{x}_i) - \boldsymbol{Q}(\boldsymbol{x}_i)\boldsymbol{k_e}\|. \tag{17}$$

In this method, the arbitrary vector $\boldsymbol{k_e}$ that minimizes the object function shown in Eq. (17) is determined to shape the end-point trajectory.

In this method, the minimum solution of the object function $f(\boldsymbol{k_e})$ is calculated under the following inequality constraint [21].

$$\begin{cases} \min & f(\boldsymbol{k_e}) \\ \text{subject to} & h_l(\boldsymbol{k_e}) \le 0 \quad (l = 1, 2, \ldots, 12). \end{cases} \tag{18}$$

where $h_l(\boldsymbol{k_e})$ represents the elements of a function $\boldsymbol{h}(\boldsymbol{k_e})$, and the function $\boldsymbol{h}(\boldsymbol{k_e})$ is defined by

$$\boldsymbol{h}(\boldsymbol{k_e}) = \begin{bmatrix} -(\boldsymbol{I}_6 - \boldsymbol{W}(\boldsymbol{x}_d(t))^{+}\boldsymbol{W}(\boldsymbol{x}_d(t)))\,\boldsymbol{k_e} \\ (\boldsymbol{I}_6 - \boldsymbol{W}(\boldsymbol{x}_d(t))^{+}\boldsymbol{W}(\boldsymbol{x}_d(t)))\,\boldsymbol{k_e} - \boldsymbol{v}_{\max} \end{bmatrix}, \tag{19}$$

$$\boldsymbol{v}_{\max} = v_{\max}\,[\ 1.0 \quad 1.0 \quad 1.0 \quad 1.0 \quad 1.0 \quad 1.0\ ]^{\mathrm{T}}. \tag{20}$$

where $v_{\max}$ represents the output limit of muscular tension (because the muscular tension is set to this output limit in the experiment device). Further, the muscle of the musculoskeletal system can generate only tensile force. Each muscular internal force v_j $(j = 1, 2, \ldots, 6)$ needs to satisfy the following inequality if the tensile direction is set as positive.

$$0 \le v_j \le v_{\max}. \tag{21}$$

The proposed method includes the augmented Lagrangian function for constrained minimization problems as shown in Eq. (18) and converts it to an unconstrained optimization problem. Then, the minimum solution of the object function is calculated using the Nelder–Mead method [21].

Calculation of desired joint torque

The desired joint torque $\boldsymbol{\tau}_d(\boldsymbol{x}_i)$ can be calculated in several ways. In the proposed method, the torque is computed by considering the effect of the inertia of the musculoskeletal system and setting the valid desired joint torque. The desired end-point trajectory $\boldsymbol{x}_d(t)$ is planned to move from the stationed state at the initial position $\boldsymbol{x}_0$ to the stationed state at the desired position $\boldsymbol{x}_f$. Moreover, the desired end-point trajectory $\boldsymbol{x}_d(t)$ required to achieve linear acceleration is given by

$$\boldsymbol{x}_d(t) = (\boldsymbol{x}_f - \boldsymbol{x}_0)\left\{-2\left(\frac{t}{T}\right)^3 + 3\left(\frac{t}{T}\right)^2\right\} + \boldsymbol{x}_0. \tag{22}$$

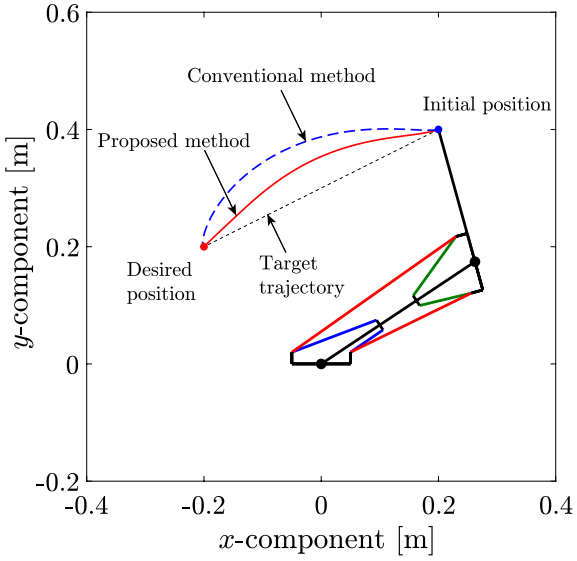

Fig. 4 End-point trajectory results for the proposed and conventional methods

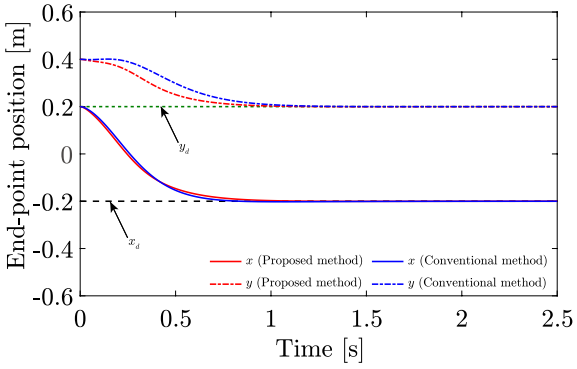

Fig. 5 Longitudinal data of the end-point position for the proposed and conventional methods

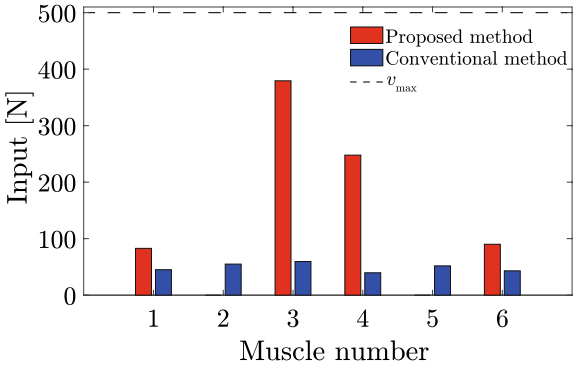

Fig. 6 Control input of the proposed and conventional methods

The desired end-point trajectory shown in Fig. 3 is divided into n, and any end-point position $\boldsymbol{x}_i$ is represented by

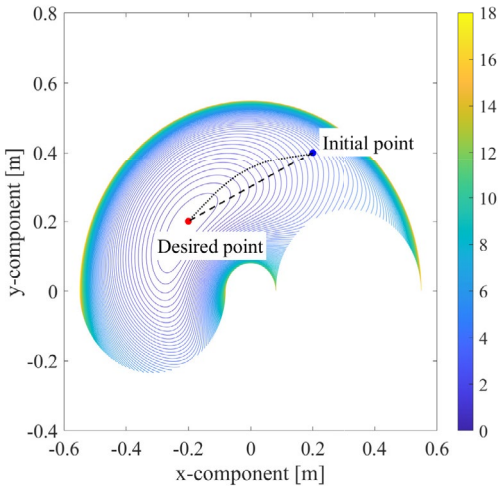

(a) Potential field of proposed method and comparison of the end-point and desired trajectories.

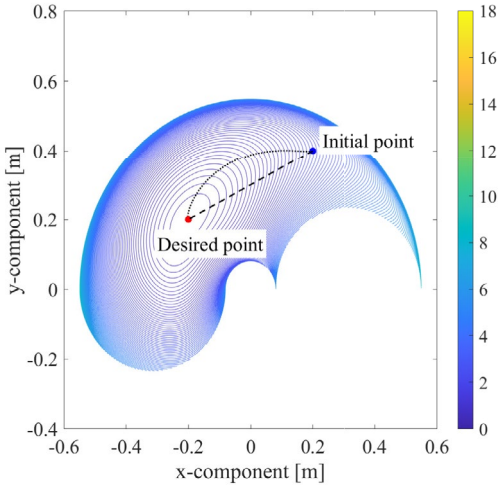

(b) Potential field of the conventional method and comparison of the end-point and desired trajectories.

Fig. 7 Potential fields generated by the control input

$$\boldsymbol{x}_i = \boldsymbol{x}_d\left(\frac{iT}{n}\right). \tag{23}$$

By differentiating Eq. (22) with respect to time, the desired trajectory of the end-point velocity $\dot{\boldsymbol{x}}_d(t)$ can be given as

$$\dot{\boldsymbol{x}}_d(t) = (\boldsymbol{x}_f - \boldsymbol{x}_0)\left(-\frac{6}{T^3}t^2 + \frac{6}{T^2}t\right). \tag{24}$$

Then, by differentiating Eq. (24) with respect to time, the desired trajectory of the end-point velocity $\ddot{\boldsymbol{x}}_d(t)$ can be given as

$$\ddot{\boldsymbol{x}}_d(t) = (\boldsymbol{x}_f - \boldsymbol{x}_0)\left(-\frac{12}{T^3}t + \frac{6}{T^2}\right). \tag{25}$$

The information of task space $\boldsymbol{x}_d(t)$, $\dot{\boldsymbol{x}}_d(t)$, and $\ddot{\boldsymbol{x}}_d(t)$ are converted into the information of the joint space $\boldsymbol{\theta}_d(t)$, $\dot{\boldsymbol{\theta}}_d(t)$, and $\ddot{\boldsymbol{\theta}}_d(t)$ using the inverse relationship of Eqs. (6)–(8).

According to the converted trajectory $\boldsymbol{\theta}_d(t)$, $\dot{\boldsymbol{\theta}}_d(t)$, $\ddot{\boldsymbol{\theta}}_d(t)$, and Eq. (9), the desired joint torque at any end-point position is represented by

$$\boldsymbol{\tau}_d(\boldsymbol{x}_i) = \boldsymbol{M}(\boldsymbol{\theta}_d(t))\ddot{\boldsymbol{\theta}}_d(t) + \boldsymbol{h}(\boldsymbol{\theta}_d(t), \dot{\boldsymbol{\theta}}_d(t)) + \boldsymbol{D}\dot{\boldsymbol{\theta}}_d(t). \tag{26}$$

Table 3 Eight desired end-point positions and each arrival time T

	x [m]	y [m]	T [s]
$\boldsymbol{x}_A$	−0.094	0.406	1.0
$\boldsymbol{x}_B$	−0.200	0.450	0.08
$\boldsymbol{x}_C$	−0.306	0.406	1.4
$\boldsymbol{x}_D$	−0.350	0.300	1.4
$\boldsymbol{x}_E$	−0.306	0.194	1.4
$\boldsymbol{x}_F$	−0.200	0.150	0.7
$\boldsymbol{x}_G$	−0.094	0.194	1.4
$\boldsymbol{x}_H$	−0.050	0.300	1.4

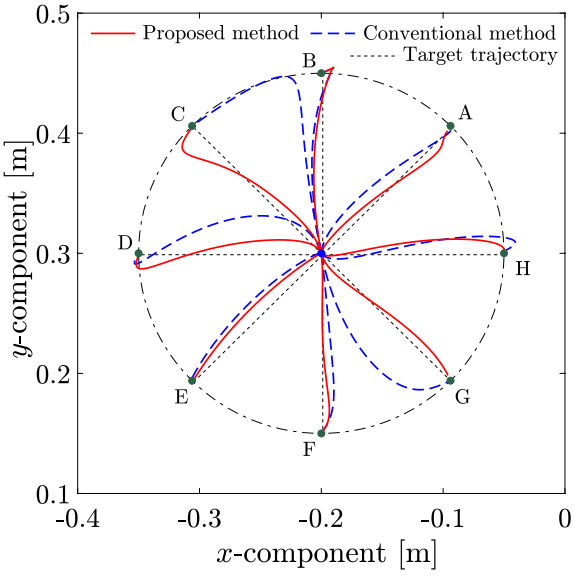

Fig. 8 Results of the control of the end-point trajectory for eight directions

Numerical simulation

In this section, the effectiveness of the proposed method is confirmed through numerical simulations of positioning for the musculoskeletal system shown in Fig. 1. In this simulation, the musculoskeletal system is controlled from the initial end-point position $\boldsymbol{x}_0 = [0.2,\ 0.4]^{\mathrm{T}}$ [m] to the desired end-point position $\boldsymbol{x}_f = [-0.2,\ 0.2]^{\mathrm{T}}$ [m], and the results of the proposed method are compared with that of the conventional method (PTP control). Tables 1 and 2 list the physical parameters of the musculoskeletal system obtained using the simulation and the muscular arrangement of the musculoskeletal system, respectively.

In the proposed method, the output restriction value is set to $v_{\max} = 500$ [N], number of the end-point position is set to $n = 4$, and arrival time is set to $T = 0.5$ [s]. The desired joint torque at any end-point position is determined using the computed torque method under these conditions. The optimized arbitrary vector obtained using the proposed method is given by

$$\boldsymbol{k_e} = \begin{bmatrix} -1554.08 \\ 1636.89 \\ 1471.83 \\ -944.12 \\ -944.12 \\ -810.54 \end{bmatrix}. \tag{27}$$

The arbitrary vector of the conventional PTP control method is determined using the following vector sets to obtain the same 5% setting times.

$$\boldsymbol{k_e} = 50\,[\ 1.0 \quad 1.0 \quad 1.0 \quad 1.0 \quad 1.0 \quad 1.0\ ]^{\mathrm{T}}. \tag{28}$$

The results of the simulation are presented in Figs. 4, 5 and 6 and those of the end-point trajectory in the task space are shown in Fig. 4. The time series data of the end-point position are shown in Fig. 5, and the control input is shown in Fig. 6. The proposed method does not accurately follow the desired trajectory; it reduces the bulge of the end-point trajectory in contrast to that obtained with the conventional method, as shown in Fig. 4. The arrival time used for calculating the desired torque is set as $T = 0.5$ [s]; however, the simulation result does not converge at the specified time because the optimized arbitrary vector realizes the desired torque due to the features of the musculoskeletal system. The end-point position cannot perfectly track the desired trajectory, hindering the achievement of the target arrival time. In the proposed method, the arrival time is used to adjust the tracking performance and responsiveness owing to its influence on the desired torque. Additionally, as shown in Fig. 5, both those results show equivalent convergence times. The responsiveness can be evaluated using this convergence time. Notably, the proposed method is that it can shape the end-point trajectory based on the desired trajectory. However, accurately following the desired trajectory is challenging because of the characteristics of muscular internal force feedforward positioning, as described Section 4.

As shown in Fig. 6, the proposed method can shape the end-point trajectory in the limitation because the control input satisfies Eq. (21). Previous researchers [22, 23] used a sensor to consider the output limit of muscular tension, whereas the proposed method circumvents the use of sensors.

The potential field generated by each control input is shown in Fig. 7. The potential value $P = 0$ at the desired position, with the stable equilibrium at this point due to muscular arrangements [9] converging there. As shown in Fig. 7a, while the potential value increases, the shape of the potential field cannot change drastically. From the desired position, the U-shaped valley of the contour-line approaches the desired trajectory. Therefore, the proposed method shapes the end-point trajectory. Previous research [17] set the desired trajectory in joint space,

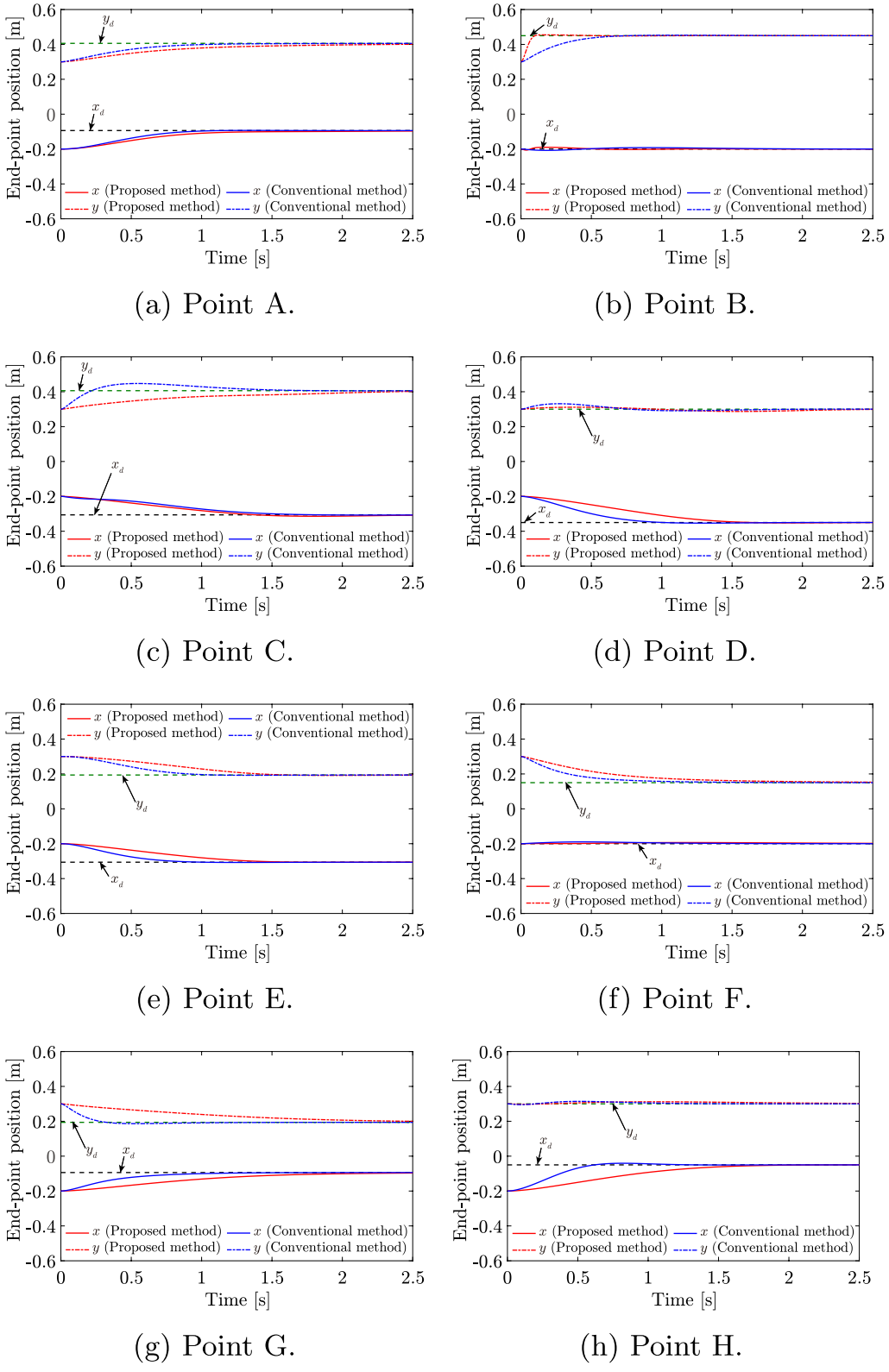

Fig. 9 Comparison of the longitudinal data of the end-point position from the initial position to eight desired positions of the proposed and conventional methods

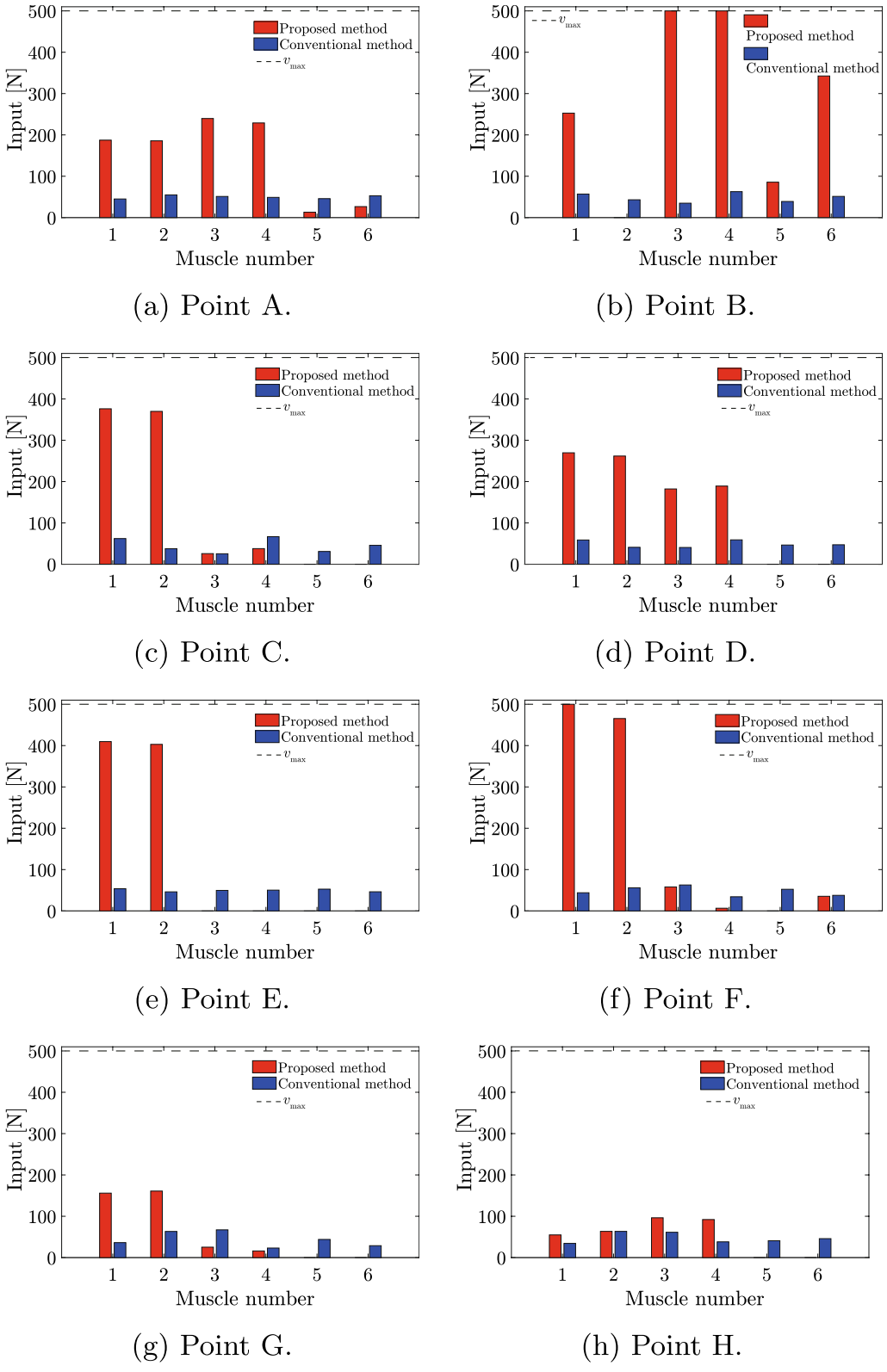

Fig. 10 Comparison of the control inputs from the initial position to the eight desired positions of the proposed and conventional methods

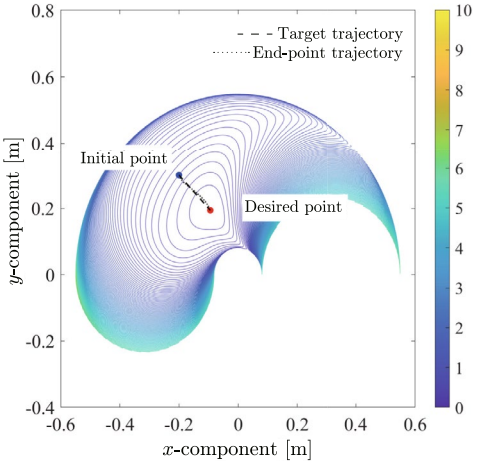

(a) Relationship between the end-point trajectory and the potential field using the proposed method.

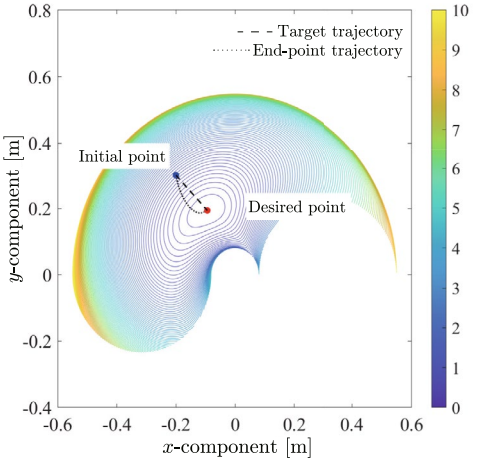

(b) Relationship between the end-point trajectory and the potential field using the conventional method.

Fig. 11 Comparison of the shape of the potential field and end-point trajectory at G of the proposed and conventional methods

while the proposed method sets it in the task space as a practical approach.

The advantage of the proposed method is that the end-point trajectory can be shaped based on desired trajectory while considering output limit. The objective function in Eq. (17) does not include a responsiveness index, which could deteriorate responsiveness or cause vibrations. The responsiveness can be adjusted by changing the arrival time T or number of end-point position n.

Evaluation of directional dependency

Simulations are performed to control the end-point position as it moved from the initial position to the eight desired positions to evaluate the directional dependency of the proposed method. In these simulations, the initial position is set to $\boldsymbol{x}_0 = [-0.2,\ 0.3]^{\mathrm{T}}$ [m], and the eight desired positions are set at equal intervals on a circumference of a circle with a radius 0.15 [m]; the center is set as the initial position. Each desired position is listed in Table 3.

The result of the end-point trajectory in the task space is shown in Fig. 8; the time series data of the end-point position are shown in Fig. 9; the control input is shown in Fig. 10. In this simulation, the results of the proposed method are compared with the conventional method (PTP control) using the arbitrary vector shown in Eq. (28). The arrival time T is set to obtain a high tracking performance and the same responsiveness of PTP control using the arbitrary vector shown in Eq. (28). However, the tracking performance became poor at point B when we focused on the same responsiveness. As the purpose of the proposed method is to shape the end-point trajectory based on the desired trajectory, the arrival time T is set to obtain a high tracking performance at point B. Therefore, the result of point B is better than the PTP control and the arrival time T is much shorter than at the

other points. The parameters of the simulations are listed in Table 3.

As shown in Fig. 8, the result of the proposed method can reduce the bulge of the end-point trajectory in contrast to that with the conventional method and shape of the end-point trajectory. The conventional method shows different end-point trajectories based on the directions of the desired positions; however, using the proposed method, the end-point trajectory can be shaped according to the desired trajectory without depending on the directional dependency. Each result confirms the equivalency of responsiveness (Fig. 9), and the restriction condition of the control input is satisfied (Fig. 10).

At point G, attention is focused because the end-point trajectory follows the desired trajectory, significantly modified from conventional results. The proposed method requires larger control input compared to the conventional method at point G. However, the potential field in Fig. 11 becomes smaller than the conventional method. This occurs because the proposed method shapes the end-point trajectory to follow the desired path. The potential field can be drastically changed to shape the desired trajectory (Fig. 11).

Conclusion

In this study, we proposed a novel method for shaping the end-point trajectory in musculoskeletal systems by optimizing an arbitrary vector using the objective function of the joint torque at any end-point position in muscular internal force feedforward positioning. Enhancing the trajectory tracking performance based on muscular internal force feedforward positioning for the musculoskeletal system is challenging. However, the end-point trajectory can be shaped based on the desired trajectory without directional dependency. The proposed method prevents the output limit of muscular tension without sensors. One approach to increase effectiveness is combining the method with a musculoskeletal system with variable joint stiffness mechanisms [24]. This system can enhance trajectory tracking by altering muscular arrangements during movement. Future investigations will be focus on examining this combination in detail.

Acknowledgements
This work was supported by JSPS KAKENHI Grant Numbers JP21K17835, JP24K15131.

Author contributions
Y. M. conducted the research concept, wrote the main manuscript text. All research and simulations are conducted by Y. M., K. T. and H. K. All authors reviewed the manuscript.

Data availability
No datasets were generated or analysed during the current study.

Declarations

Competing interests
The authors declare no Competing interests.

Received: 9 November 2025 / Accepted: 24 February 2026
Published online: 10 April 2026

References

1. Wittmeier S, Alessandro C, Bascarevic N et al (2013) Toward anthropomimetic robotics: development, simulation, and control of a musculoskeletal torso. Artif Life 19(1):171–193. https://doi.org/10.1162/ARTL_a_00088
2. Jantsch M, Schmaler C, Wittmeier S, et al. (2011) A scalable joint-space controller for musculoskeletal robots with spherical joints. Proc. of the 2011 IEEE. Int Conf on Robotics and Biomimetics. pp 2211–2216
3. Mizuuchi I, Yoshikai T, Sodeyama Y, et al (2006) Development of musculoskeletal humanoid kotaro. In: Proc. of the 2006 IEEE Int Conf on Robotics and Automation. pp 82–87
4. Mizuuchi I, Nakanishi Y, Sodeyama Y, et al (2007) An advanced musculoskeletal humanoid Kojiro. In: Proc of the 2007 7th IEEE-RAS Int Conf on Humanoid Robots. pp 294–299
5. Asano Y, Mizoguchi H, Kozuki T, et al (2013) Achievement of twist squat by musculoskeletal humanoid with screw-home mechanism. Proc. of the 2013 IEEE/RSJ Int Conf on Intelligent Robots and Systems, 4649–4654
6. Asano Y, Nakashima S, Kozuki T, et al (2016) Human mimetic foot structure with multi-dofs and multi-sensors for musculoskeletal humanoid kengoro. Proc. of the 2016 IEEE/RSJ Int Conf on Intelligent Robots and Systems. pp 2419–2424
7. Morizono T, Furusawa K, Kino H (2024) Investigation of the possibility of high-speed motion of a non-pulley musculoskeletal robot. J Robot Mechatron 36(5):1284–1290. https://doi.org/10.20965/jrm.2024.p1284
8. Kino H, Kikuchi S, Yahiro T, et al (2009) Basic study of biarticular muscle's effect on muscular internal force control based on physiological hypotheses. Proc. of the 2009 IEEE Int Conf on Robotics and Automation. pp 4195–4200
9. Kino H, Kikuchi S, Matsutani Y et al (2013) Numerical analysis of feedforward position control for non-pulley musculoskeletal system: a case study of muscular arrangements of a two-link planar system with six muscles. Adv Robot 27(16):1235–1248. https://doi.org/10.1080/01691864.2013.824133
10. Tahara K, Kuboyama Y, Kurazume R (2012) Iterative learning control for a musculoskeletal arm: Utilizing multiple space variables to improve the robustness. In: Proc. of the 2012 IEEE/RSJ Int Conf on Intelligent Robots and Systems. pp 4620–4625
11. Blana D, Kirsch RF, Chadwick EK (2009) Combined feedforward and feedback control of a redundant, nonlinear, dynamic musculoskeletal system. Med Biol Eng Comput 47:533–542. https://doi.org/10.1007/s11517-009-0479-3
12. Liu S, Wang Y, Zhu Q (2007) A trajectory tracking control scheme of a human arm in the sagittal plane. Proc. of the 2007 Int Conf on Mechatronics and Automation. pp 3295–3299
13. Katayama M, Kawato M (1990) Learning trajectory and force control of an artificial muscle arm by parallel-hierarchical neural network model. Proc. of the 1990 Conf. Adv Neural Inf Process Syst 3:436–442
14. Kawato M, Gomi H (1992) A computational model of four regions of the cerebellum based on feedback-error learning. Biol Cybern 68:95–103. https://doi.org/10.1007/BF00201431
15. Arimoto S (1996) Control theory of non-linear mechanical system: a passivity-based and circuit-theoretic approach. Clarendon Press, Oxford
16. Wang A, Mingcong D (2010) Human arm-like robot control using the visco-elasticity of human multi-joint arm. In: Proc. of the 5th Int Conf on Computer Sciences and Convergence Information Technology. pp 738–743
17. Kinjo Y, Matsutani Y, Tahara K et al (2023) Basic study of sensorless path tracking control based on the musculoskeletal potential method. ROBOMECH J 10:3. https://doi.org/10.1186/s40648-023-00242-2
18. Senda K, Komada K, Morizono T, et al (2024) Proposal of feedforward trajectory control with iterative learning for a musculoskeletal system. In: Proc. of the 2024 IEEE 18th Int Conf on Advanced Motion Control. pp 1–5
19. Yoshikawa T (1990) Foundations of Robotics: analysis and Control. The MIT Press, London
20. Kino H, Ochi H, Matsutani Y et al (2017) Sensorless point-to-point control for a musculoskeletal tendon-driven manipulator: analysis of a two-dof planar

system with six tendons. Adv Robot 31(16):851–864. https://doi.org/10.1080/01691864.2017.1372212
21. Hirai S (2019) Numerical Methods for Mechanical Systems: MATLAB Version. Corona Publishing Co., Ltd., Tokyo (**in Japanese**)
22. Matsutani Y, Tahara K, Kino H (2019) Set-point control of a musculoskeletal system under gravity by a combination of feed-forward and feedback manners considering output limitation of muscular forces. J Robot Mechatron 31(4):612–620. https://doi.org/10.20965/jrm.2019.p0612
23. Tahara K, Matsutani Y, Nakagawa D, et al (2016) Variable combination of feed-forward and feedback manners for set-point control of a musculoskeletal arm considering the maximum exertable muscular force. In: Proc. of the 42th Annual Conf of the IEEE Industrial Electronics Society. pp 815–820
24. Matsutani Y, Tahara K, Kino H, et al (2017) Stiffness evaluation of a tendon-driven robot with variable joint stiffness mechanisms. In: Proc. of the IEEE-RAS 17th Int Conf on Humanoid Robotics. pp 213–218

Publisher's Note